Role of Conformation in the Electronic Properties of Chemisorbed Pyridine on Cu(110): An STM/STS Study

D. B. Dougherty, J. Lee, and J. T. Yates, Jr.*

Surface Science Center and Department of Chemistry, University of Pittsburgh, Pittsburgh, Pennsylvania 15260

Received: February 3, 2006; In Final Form: April 11, 2006

Pyridine was chemisorbed on Cu(110) at 10 K and observed using STM at 5 K as dosed and after annealing to temperatures between 20 and 300 K. At very low coverage, two molecular species with different apparent heights are observed to coexist. The higher species is assigned to a pyridine molecule bonded with its symmetry axis perpendicular to the surface plane, while the lower species is assigned to a pyridine molecule that is tilted down toward the surface plane. At low coverage, the tilted pyridine species predominates on the surface, but as the total surface coverage of pyridine increases, the molecules stand up until the upright geometry becomes favored. Measurements of the STS of the two species show different molecular resonances derived from the lowest unoccupied pyridine π^* orbitals. The tilted pyridine species has a peak in the unoccupied local density of states at 2.6 ± 0.1 eV, whereas the upright pyridine species has a peak at 2.3 ± 0.1 eV.

I. Introduction

Pyridine (C_5H_5N, Figure 1a) is a prototype molecule for understanding the delicate forces governing chemisorption on metal surfaces. Isolated pyridine has two essential features: (1) a π electron system similar to that of benzene; and (2) a nonbonding lone pair of electrons associated with the heterocyclic N atom, similar to that present in ammonia. The interplay between these two features leads to several possible chemisorption modes on a metal surface. In one extreme, the molecule may bind entirely through the lone-pair electrons with its plane perpendicular to the surface plane (see Figure 1b). In another, it may bind entirely through the π electron system with its plane parallel to the surface plane. These possibilities are referred to as N-bonding and π-bonding, respectively, and have been reported for pyridine adsorption on several metals.[1−18] Intermediate cases where the molecular plane is tilted and/or twisted with respect to the surface normal are also possible as illustrated schematically in Figure 1c.

The situation for most metals is that the bonding geometry of pyridine is a function of temperature and coverage.[1−18] For example, on Pt(111) a reflection absorption infrared spectroscopy (RAIRS) study[4] has shown that pyridine initially adsorbs either tilted or as a mixture of tilted and N-bonded species. Upon increasing the surface coverage, the molecule shows a complicated tilting and twisting, presumably due to crowding effects.[4] On Cu(111), a similar coverage-induced change from π-bonding or tilting to N-bonding has been reported on the basis of two photon photoemission (2PPE) and temperature programmed desorption (TPD) observations.[18]

The Cu(110) surface is unique from the standpoint of pyridine adsorption in that the pure N-bonding configuration has been reported to be present for all coverages and temperatures.[1−6] In fact, although there is probably a favorable interaction between the π electrons in pyridine and any metal surface, there is no reported evidence that this interaction is strong enough to influence the adsorption configuration on Cu(110). Experiments employing techniques such as angle-resolved ultraviolet photoemission (ARUPS),[1−3] RAIRS,[4] photoelectron diffraction (PhD),[5] and electron stimulated desorption ion angular distribution (ESDIAD)[6] have been interpreted as ruling out a π-bonding contribution to the geometry of pyridine on this surface.

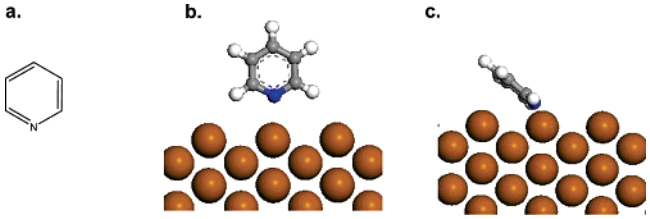

Figure 1. (a) Schematic of the pyridine molecule. (b) Schematic of an N-bonded pyridine molecule on a surface. (c) Schematic of a π-bonded pyridine molecule on a surface.

The present work describes low-temperature STM observations that show a tilted or π-bonded adsorption configuration is favored on Cu(110) at *extremely* low coverage. In addition, the observations show that there is a transition from predominant tilting (or π-bonding) to predominant N-bonding as the pyridine coverage increases and that the bonding configurations have significantly different molecular resonances in the unoccupied local density of states.

Understanding this chemisorption system has two values. First, it is important to note that the π electron system in pyridine is significantly involved in the bonding to the surface at low coverage. In this way Cu(110) and Cu(111) are similar with respect to the coverage-dependent pyridine adsorption configuration,[17,18] and indeed Cu(110) is similar to many other metal surfaces on which chemisorbed pyridine exhibits an orientational transition as a function of coverage.[4,8,12,18] Second, the dramatic effect of molecular orientation on the local density of states is an unexpected observation. It is an important addition to the present body of knowledge about surface electronic structure that may be particularly relevant to the active fields of organic and molecular electronics.[19−20]

II. Experimental Methods

A single-crystal Cu(110) crystal (MaTeck, orientation accuracy ±0.5°) was cleaned in a UHV preparation chamber (base

* Corresponding author.

10.1021/jp060733r CCC: $33.50
Published on Web 06/01/2006

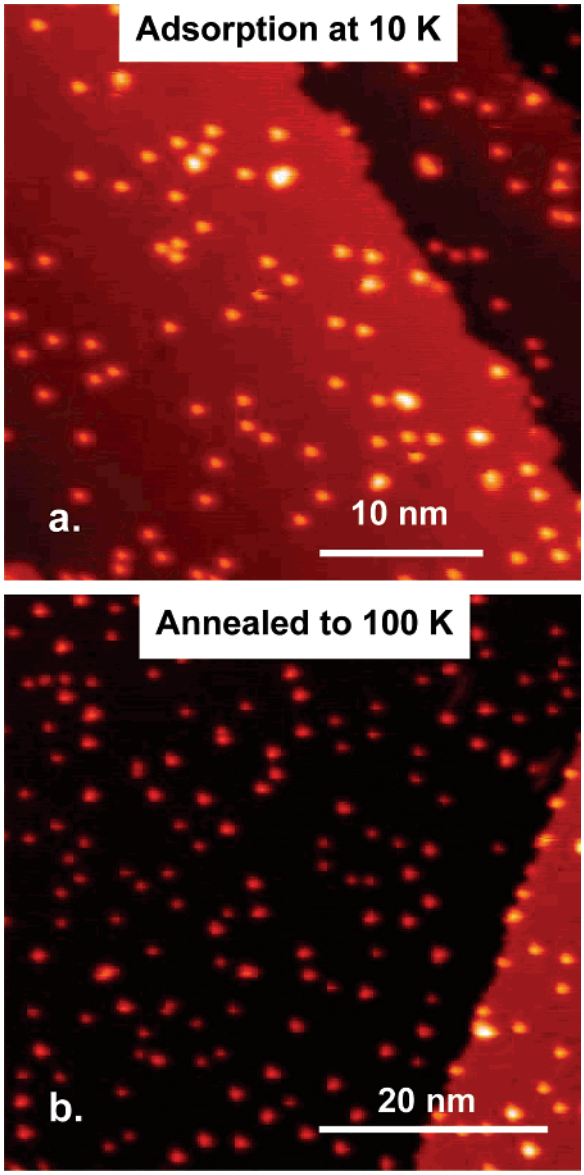

Figure 2. (a) STM image (34.95 nm × 34.95 nm, −1.0 V, 0.074 nA) obtained at 5 K immediately after dosing pyridine at a crystal temperature of 10 K; (b) STM image (50 nm × 50 nm, −1.0 V, 0.076 nA) after annealing the surface in part (a) to approximately 100 K.

pressure ≈ 1×10^{-9} mbar) by repeated cycles of sputtering with 1 keV Ar^+ ions followed by annealing to ∼800 K. The crystal was transferred through a gate valve to an STM chamber (base pressure < 1×10^{-10} mbar) that houses a commercial low-temperature STM (LT-STM, Omicron). The crystal was cooled to 5 K for imaging, and its temperature rose to 10 K during pyridine dosing. Pyridine was purified by several freeze−pump−thaw cycles and dosed through a translatable stainless steel tube onto the Cu(110) crystal held in the cold STM stage. The only minor surface impurity observable by AES was carbon, and its coverage was estimated to be 1−3% of a Cu(110) layer (density 1.1×10^{15} cm^{-2}) by direct STM observation after cleaning.

The sample could be annealed to temperatures between 20 and 300 K by removing it from the STM stage and either holding it in a wobble stick for 1−3 min (up to 100 K) or placing it in a room-temperature sample carousel (100−300 K). The temperatures attainable by these procedures were calibrated on the basis of experience with the thermal desorption and diffusion of several molecules. The wobble stick heating rate was

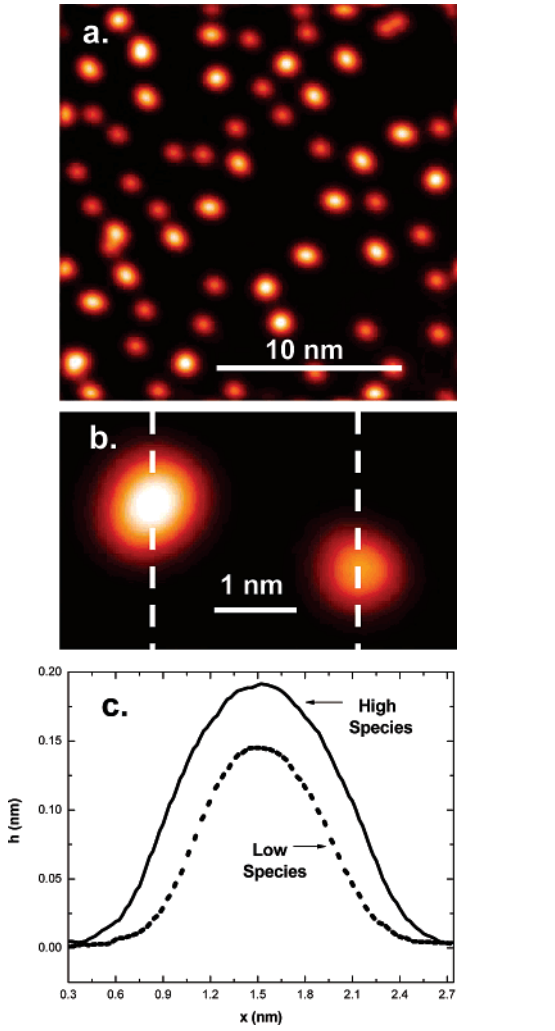

Figure 3. (a) STM image (21.42 nm × 21.42 nm, +1V, 0.08 nA) of a surface dosed with pyridine at 10 K and then annealed to 100 K; (b) high magnification STM image (4.73 nm × 2.83 nm, +0.5 V, 0.076 nA) of the two different pyridine species on the surface; (c) line profiles extracted from the STM images along the dashed lines in part (b).

calibrated on the basis of the approximate ordering temperature of methanethiol on Au(111).[21] The heating rate in the sample carousel was approximately calibrated by depositing a multilayer film of pyridine on the Cu(110) crystal and observing its desorption (at 160 K[6]) using the total pressure reading from the chamber's ion gauge.

STM topography was measured in constant current mode with homemade electrochemically etched tungsten tips. Tips were processed in situ by voltage ramps from −10 to +10 V with the feedback disengaged. Tunneling currents ranged from ∼30 up to 500 pA, and gap voltages for imaging were typically between −3.0 and +1.0 V. Scanning tunneling spectroscopy (STS) was performed by modulating the tunneling gap voltage with a sine wave whose amplitude was set between 7 and 200 mV and whose frequency was set between 400 and 700 Hz. A digital lock-in amplifier (Stanford Research Systems 830) was then used to detect the first harmonic of the resulting tunneling current while the tip−sample DC bias was swept over the desired range with the feedback loop off.

III. Experimental Results

III. A. STM Topography. Deposition of pyridine at 10 K produces the random distribution of molecular features shown in Figure 2a. The molecules apparently remain where they land

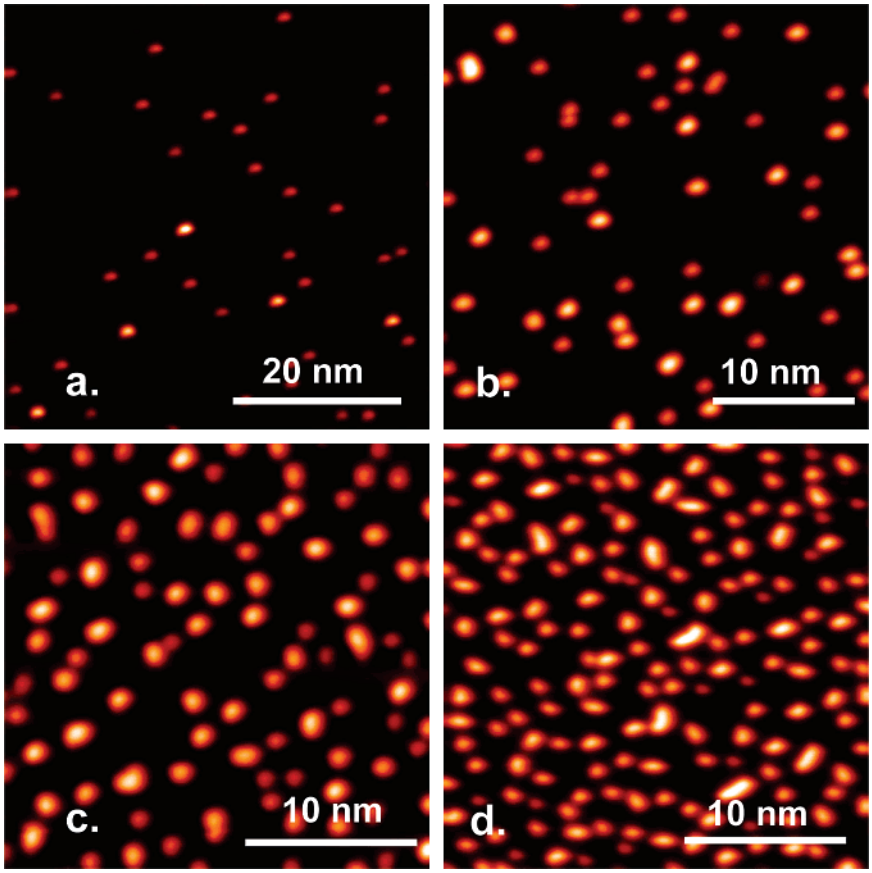

Figure 4. Sequence of STM images obtained at 5 K following adsorption at 10 K and annealing to 100 K for increasing pyridine surface coverage; (a) total coverage of 0.017 nm^{-2} (50 nm × 50 nm, +1 V, 0.05 nA); (b) total coverage of 0.071 nm^{-2} (29.98 nm × 29.98 nm, −0.5 V, 0.1 nA); (c) total coverage of 0.148 nm^{-2} (24.52 nm × 24.52 nm, −1.0 V, 0.06 nA); (d) total coverage of 0.198 nm^{-2} (26.13 nm × 26.13 nm, +0.9 V, 0.05 nA).

upon arriving from the gas phase and show no clear preference even for atomic step defects present about every 50 nm on the surface. By annealing the surface to ~100 K, the only change that is observed in the image shown in Figure 2b is that the step sites become preferentially occupied. Clearly, the molecules have enough mobility at 100 K[22] to diffuse to the more active step sites where they are then strongly bound. On the terraces, the arrangement of molecular features remains essentially random even after this annealing step. Further annealing of the surface up to 300 K does not result in significant changes in the overall distribution of molecules on the surface compared to that in Figure 2b except that at room temperature desorption occurs at a rate that leaves the crystal nearly clean in about 2−3 h.

Inspection of Figure 2 shows that there are actually two molecular features on the surface with different apparent heights. In Figure 3a another example of a deposition of pyridine at 10 K followed by annealing to 100 K is shown. Here the two apparent heights are also clearly seen. Figure 3b shows a magnified image of the two different height species, side by side. Line profiles taken through the centers of each species in Figure 3b (marked by dashed white lines) are given in Figure 3c. By making a sampling of the heights of molecular features from many similar images obtained in the course of several different STM experiments, the average height of the high species is 0.186 ± 0.006 nm, whereas the average height of the low species is 0.142 ± 0.005 nm.

III. B. Coverage-Dependent STM Topography. At extraordinarily low pyridine coverage, mostly "low" species are observed on the surface. This can be seen in Figure 4a where only a few high species can be found. Upon slightly increasing the pyridine surface coverage from this point, both low and high molecular species can be found readily as shown in Figure 4b. At this low coverage, the lower apparent height species are still the clear majority species on the surface. When the coverage is increased beyond that shown in Figure 4b, it is found that the proportion of high species tends to increase. In Figure 4c, a nearly equal number of high species and low species coexists, while in Figure 4d high species are the majority species[23] and only a few low species can be found. Qualitatively visible in the sequence in Figure 4 is the gradual change from a majority of low molecular species to a majority of high molecular species at 100 K.

The change in majority height with coverage was quantified by counting the number per unit area of each apparent height species in STM images obtained after 13 differing pyridine exposures. In Figure 5a, the surface concentration of low species (c_{low}) is plotted as a function of the *total* surface concentration of molecules (c_{total}). In Figure 5b, the coverage of high species is plotted as a function of total coverage. The graphs in Figure 5 illustrate the abrupt change in the preferred orientation of the surface species as a function of coverage. Initially, the coverage of both apparent types of species grows with the total number of molecules per unit area, and the rate of growth of concentration of the low species is somewhat higher than the rate of growth of the concentration of high species. At a coverage of approximately 0.1 nm^{-2}, the coverage of low species begins to drop and to approach zero, whereas, the coverage of high species begins to grow with increasing total coverage at an increased rate. While the data presented in Figure 5 correspond to an

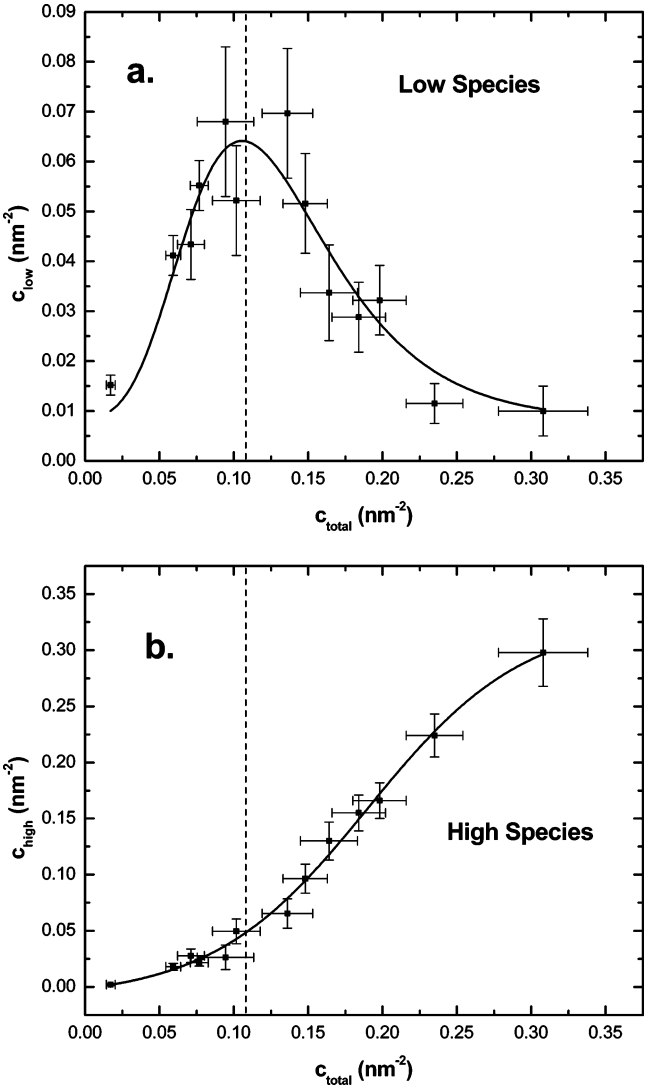

Figure 5. (a) Coverage of lower apparent height pyridine species as a function of total surface concentration. (b) Coverage of higher apparent height pyridine species as a function of total surface concentration. The dashed line marks the approximate total pyridine coverage at which the low species begins to decrease in number and the rate of growth of the coverage of high species increases. The solid lines in both plots are guides to the eye.

annealing temperature of 100 K, the distribution of different pyridine species did not change after briefly annealing to 300 K.

III. C. Local Tunneling Spectroscopy. The two pyridine species at very low coverage can be distinguished not only by their different apparent heights but also by their different spectroscopic characteristics. Figure 6 shows examples of tunneling spectra between ±3 V for both types of pyridine species as well as for the Cu(110) substrate. The important points from Figure 6 are that, in the occupied states (i.e. $V < 0$), there are no distinguishing features in the STS behavior for the low and high pyridine species. In the unoccupied states however, the spectra for the molecules have onset-like features around 2 eV that are not present in the substrate spectra. More importantly, the onset occurs at a lower voltage for the high pyridine species than for the low pyridine species.

The differences between the STS measurements can be seen more clearly in Figure 7a, which shows tunneling spectra obtained for the unoccupied states for the voltage range from 1 to 3 V. In this figure, the spectra are plotted in normalized units

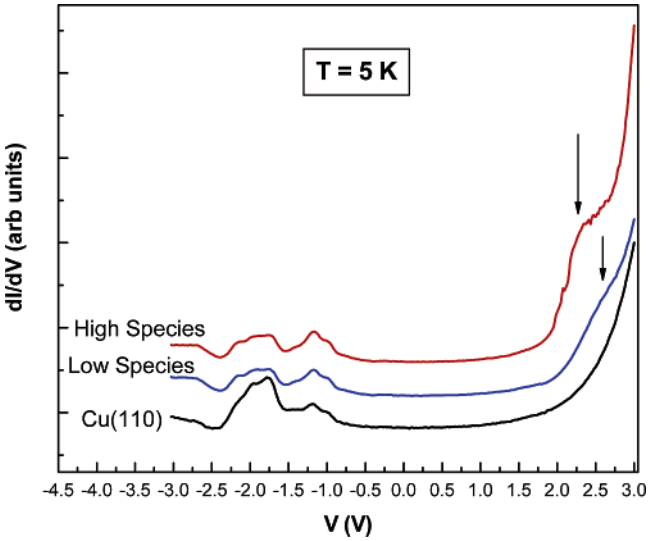

Figure 6. Tunneling spectra measured at 5 K for the two different pyridine species and the bare Cu(110) surface (initial setpoint: −3.0 V, 0.5 nA).

([V/I] dI/dV) to reflect the density of states.[24] Here the lower onset voltage for the high species compared to the low species is easily seen. In addition, the peak in the spectra for the high species occurs at about 2.2 eV while the peak for the low species occurs at about 2.5 eV. In Figure 7b, difference spectra are plotted in which the substrate background is subtracted from each of the STS measurements in Figure 7a.

The onset of the resonance in the unoccupied states for the high pyridine species was always observed to start at or below 2 eV. The precise position of the onset was somewhat variable, however. Comparing one spectrum to another, the onset was sometimes observed to occur at voltages as low as 1.5 eV. In addition, the spectra for the high species tended to be noisy for voltages after the onset (note in particular Figure 6). In contrast, the spectra obtained for the low species were less noisy at all voltages and had a significantly more reproducible onset.

The differences in the local density of states of the chemisorbed pyridine species that are illustrated in Figures 6 and 7 were reproducible over many experiments with moderate variations in tunneling conditions and using different STM tips. Based on 21 averaged spectra similar to those presented in Figures 6 and 7, the average peak position for the high pyridine species is found to be 2.3 ± 0.1 eV. The individual spectra averaged to obtain these results were made by averaging 3−20 dI/dV individual scans for different molecules in the same local area and the uncertainty is taken as the standard deviation of the 21 measured peak positions. In the same way, 18 averaged spectra were used to determine an average peak position for the low species of 2.6 ± 0.1 eV. The averaged spectra include dI/dV scans for well over 100 of each type of adsorbed pyridine species.

IV. Discussion

IV. A. Assignment of Different Pyridine Species. Based on bias-independent STM topography, the simplest assignment of the two species observed by STM is to pyridine molecules with different tilt angles with respect to the surface. The precise tilt angle of a molecule cannot be determined using STM, but it is known that a purely N-bonded normally oriented configuration of pyridine on Cu(110) occurs at low coverage.[6] This suggests that the pyridine species with a greater apparent height is purely N-bonded and the pyridine species with the smaller

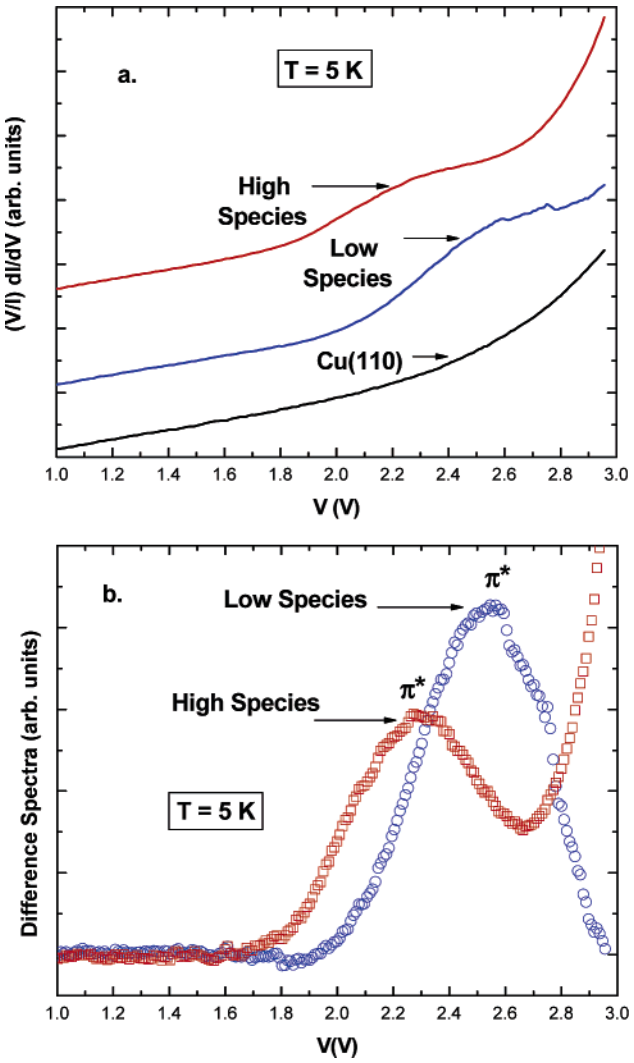

Figure 7. (a) Normalized tunneling spectra for the two different pyridine species and the Cu(110) surface (initial set point: −3.0 V, 0.3 nA); (b) difference spectra for the two pyridine species obtained from the data in part (a) by subtracting the substrate spectra from each of the tunneling spectra through a pyridine species.

apparent height is a tilted species stabilized by favorable interactions between the aromatic electrons in the molecule and the electrons in the metal.

The observation that a mixture of low and high species coexists at 10 K at very low coverage indicates that the two configurations have very similar binding energies in the limit of zero coverage. For example, for pyridine on Ag(111), thermal desorption observations indicate that the binding energy of a tilted pyridine species is less than 100 meV higher than that of an N-bonded pyridine species at higher coverage.[8] In adsorption at 10 K, the configuration produced by a collision of a pyridine molecule with the cold surface is determined by the details of the trajectory of the molecule arriving from the gas phase. The absence of a mobile precursor adsorption process at 10 K is indicated by the lack of recognition by pyridine molecules of the energetically favorable atomic step sites (Figure 2).

As mentioned in the Introduction, previous studies using a variety of experimental techniques were all interpreted as indicating only an N-bonded pyridine on Cu(110). Our measurements (Figures 4 and 5) show that the tilted pyridine species is present at extremely low coverage which naturally makes its observation difficult by spectroscopic techniques. For example, RAIRS[4] studies of the intensity of the out-of-plane bending modes of CH bonds may be thwarted by the low intensity of this mode even for substantial coverages as well as the fact that its frequency occurs near the lower limit of most infrared detectors (~650−850 cm^{-1}). Ultimately, the extraordinary spatial resolution of STM is required to establish the coexistence of different orientations of pyridine at low coverage.

IV. B. Coverage-Dependent Orientation. The orientation of a chemisorbed molecule is very often observed to depend on the surface coverage of the molecule.[4,8,12,18,25] This is usually the result of the interplay between substrate−molecule and molecule−molecule interactions. At low coverages, the orientation is determined primarily by substrate−molecule interactions while at high coverages it may change due to the increasing importance of molecule−molecule interactions. These considerations have been applied to the chemisorption of pyridine on substrates such as Ag(111),[8] Ni(001),[12] Pt(111),[4] and Cu(111).[18]

The significance of intermolecular interactions between pyridine molecules on Cu(110) has been established by Lee et al.[6] using TPD and ESDIAD measurements. First-order thermal desorption spectra for this system (exhibiting a chemisorption energy of 0.97 eV in the limit of zero coverage) show a characteristic shift in peak position to lower temperatures as the total pyridine coverage increases that is the result of repulsive intermolecular interactions. The repulsive interaction energy was measured to be 0.16 eV at one monolayer coverage. Similarly, for pyridine adsorbed on Cu(111), TPD measurements and corresponding 2PPE spectra were attributed to different surface "phases" in which molecules are in the low-coverage phase π-bonded and in the high-coverage phase N-bonded.[18]

The coverage at which the change in preferred orientation occurs for pyridine on Cu(110) is extraordinarily low, corresponding to approximately 1 molecule per 10 nm^2. This fact makes *direct* intermolecular interactions an unlikely driving force for the orientational change. Instead, an indirect, long-range interaction is probably involved in destabilizing the tilted pyridine orientation. Such a repulsive interaction has been implicated in the formation of pentacene rows on Cu(110).[26] These rows are spaced by approximately 2.8 nm, a distance that is the same order of magnitude as the typical molecule−molecule separation observed near the orientational transition for pyridine on Cu(110). The repulsion between pentacene rows has been argued[27] to arise from charge density waves created by the molecule in the (molecule-modified) two-dimensional surface-state band on Cu(110).[26] Microscopically, the origin of the repulsion between tilted pyridine molecules on Cu(110) may be similarly surface-state mediated. Direct evidence for this mechanism is lacking at present, but it is clear that a long-range interaction will be required to explain the observed transition.

IV. C. Effect of Orientation on Electronic Structure. The different conformations of the pyridine molecules on Cu(110) have significantly different electronic characteristics. The first molecular resonance in the unoccupied local density of states occurs at 2.3 ± 0.1 eV for an N-bonded species and at 2.6 ± 0.1 eV for a tilted species. The shift of 0.3 ± 0.1 eV between the energetic positions of the peaks for the two pyridine species is small when compared to the total energetic separation from the Cu(110) Fermi level (~2−3 eV) but is significant when viewed as the barrier to injection of electrons from a metal electrode.[20] A difference in barrier height of several hundred meV means that electrons are more easily injected into an N-bonded pyridine species than into a tilted pyridine species.

The low-coverage unoccupied electronic structure of chemisorbed pyridine has been of interest for many surfaces. Demuth and Sanda[8] used electron energy loss spectroscopy (EELS) to

observe a feature at 1.4 eV above the Fermi level for pyridine adsorbed on Ag(111). They described this feature as the result of the excitation of Ag d-band electrons to the lowest pyridine π^* orbital. A feature similar to that reported for pyridine/Ag(111) was reported by Zhong et al. for pyridine/Cu(111).[18] Using 2PPE, these authors observed a very weak and broad feature 1−2 eV above the Fermi level for submonolayer pyridine chemisorption and suggested that it is also due to a charge-transfer excitation.[18]

The peaks in the unoccupied density of states observed by STS for pyridine chemisorbed on Cu(110) can be assigned to to resonances derived from the lowest π^* orbital of pyridine. The position of the resonance is different for the different orientations since the π^* orbital of each hybridizes differently with the metal surface. Specifically, greater overlap with metal orbitals is expected on geometric grounds for the orbitals of a tilted pyridine than for those of an N-bonded pyridine. This enhanced overlap leads to a higher-energy "antibonding" state for the tilted pyridine species. It is likely that an excitation of Cu electrons into these states could be observed spectroscopically as in the case of pyridine chemisorbed on Ag(111)[8,10] and Cu(111).[18] Indeed the resonances reported in the present study for both types of pyridine bonding occur in an energy range similar to the range of excitation energies in refs 8 and 18. In addition, on Cu(111) for a pyridine coverage of approximately 1−2 ML, inverse photoemission has assigned a broad feature at 2.5 eV to the lowest pyridine π^* orbital.[13] The extent of interaction between the unoccupied molecular orbitals of pyridine and the electrons in the Cu(110) surface determines their modified energetic positions and can be expected to be substantially different for the tilted versus N-bonded pyridine species.

Time-dependent density functional theory calculations for pyridine N-bonded to small Cu clusters (two or four Cu atoms) show low-lying excitations in the range of 1−3 eV.[28] This agrees well with the STS results for the N-bonded species observed in the present work and the 2PPE results of Zhong et al. for pyridine on Cu(111).[18] The cluster calculations did not attempt to produce a tilted configuration of pyridine[28] and so cannot be used to understand the difference in excitation energies for N-bonded and tilted species observed by STM. Nevertheless, the fact that the calculated energies of the cluster analogue of an N-bonded pyridine span the range where molecular resonances are found is encouraging.[28]

The location of molecular resonances is important for molecular or organic electronics applications.[19,20,29] The position of unoccupied energy levels relative to an electrode Fermi level determines electron injection barriers in devices made of organic thin films. At the level of single-molecule electron transport, the position of molecular resonances determines the efficiency with which an electron is transferred across a molecule.[29] The differences in position of the π^*-derived molecular resonance for the differently oriented pyridine molecules on Cu(110) suggests the possibility of controlling the electrical properties of more technologically relevant molecular systems by finding the means to control molecular orientation.

V. Summary and Conclusions

Using low-temperature STM and STS measurements of pyridine chemisorption on Cu(110), the following results have been obtained:

(1) N-bonded and tilted pyridine species coexist on Cu(110) from extremely low total pyridine coverage. The pyridine conformation selected by an incident pyridine molecule may depend on the details of its trajectory as it enters into the adsorbed layer from the gas phase.

(2) At low coverage, the vast majority of chemisorbed pyridine molecules are tilted, but as the total coverage increases beyond about 0.1 nm^{-2}, the N-bonded pyridine species gradually becomes the majority species. This orientational change is attributed to long-range repulsions between tilted pyridine species.

(3) The N-bonded pyridine species exhibits a resonance in the unoccupied density of states at 2.3 ± 0.1 eV.

(4) The tilted pyridine species exhibits a resonance in the unoccupied density of states at 2.6 ± 0.1 eV.

(5) The difference in the energetic position of the resonance for the differently bonded pyridine species results from the differing overlap between the molecular orbitals and the Cu surface. The greater overlap of the π^* orbital with the Cu substrate results in an upward shift of about 0.3 eV for tilted pyridine species compared to that for N-bonded species.

Acknowledgment. This work was supported by the W.M. Keck Foundation through the W.M. Keck Center for Nanoscale Molecular Electronics as well as a grant from NEDO (Japan).

References and Notes

(1) Bandy, B. J.; Lloyd, D. R.; Richardson, N. V. *Surf. Sci*. **1979**, *89*, 344.
(2) Nyberg, G. L. *Surf. Sci.* **1980**, *95*, L273.
(3) Bridge, M. E.; Connolly, M.; Lloyd, D. R.; Somers, J.; Jakob, P.; Menzel, D. *Spectrochim. Acta, Part A* **1987**, *43*, 1473.
(4) Haq, S.; King, D. A. *J. Phys. Chem.* **1996**, *100*, 16957.
(5) Geibel, T.; Schaff, O.; Lindsay, R.; Baumgartel, P.; Polcik, M.; Bradshaw, A. M.; Koebbel, A.; McCabe, T.; Bridge, M.; Lloyd, D. R.; Woodruff, D. P. *J. Chem. Phys.* **1999**, *110*, 9666.
(6) Lee, J.-G.; Ahner, J.; Yates, J. T., Jr. *J. Chem. Phys*. **2001**, *114*, 1414.
(7) Netzer, F. P.; Bertel, E.; Matthew, J. A. D. *Surf. Sci*. **1980**, *92*, 43.
(8) Demuth, J. E.; Christmann, K.; Sanda, P. N. *Chem. Phys. Lett.* **1980**, *76*, 201.
(9) Demuth, J. E.; Sanda, P. N. *Phys. Rev. Lett*. **1981**, *47*, 57.
(10) Avouris, Ph.; Demuth, J. E. *J. Chem. Phys*. **1981**, *75*, 4783.
(11) Netzer, F. P.; Mack, J. U. *J. Chem. Phys*. **1983**, *79*, 1017.
(12) DiNardo, N. J.; Avouris, Ph.; Demuth, J. E. *J. Chem. Phys*. **1984**, *81*, 2169.
(13) Frank, K.-H.; Dudde, R.; Koch, E. E. *Chem. Phys. Lett*. **1986**, *132*, 83.
(14) Bader, M.; Haase, J.; Frank, K.-H.; Puschmann, A.; Otto, A. *Phys. Rev. Lett*. **1986**, *56*, 1921.
(15) Mate, C. M.; Somorjai, G. A.; Torn, H. W. K.; Zhu, X. D.; Shen, Y. R. *J. Chem. Phys*. **1987**, *88*, 441.
(16) Netzer, F. P.; Rangelov, G.; Rosina, G.; Saalfeld, H. B. *J. Chem. Phys*. **1988**, *89*, 3331.
(17) Davies, P. R.; Shukla, N. *Surf. Sci.* **1995**, *322*, 8.
(18) Zhong, Q.; Gahl, C.; Wolf, M. *Surf. Sci.* **2001**, *496*, 21.
(19) Heath, J. R.; Ratner, M. A. *Phys. Today* **2003**, *56*, 43.
(20) Kahn, A.; Koch, N.; Gao, W. *J. Polym. Sci., Part B: Polym. Chem.* **2003**, *41*, 2529.
(21) Rzeznicka, I. I.; Lee, J.; Maksymovych, P. M.; Yates, J. T., Jr. *J. Phys. Chem. B* **2005**, *109*, 15992.
(22) The high mobility of the pyridine molecule on the Cu(110) surface made STM imaging at 80 K impossible since the tip was observed to readily drag the molecules. The 5 K temperature at which all STM/STS measurements were made in this work was thus essential for stability.
(23) In parts c and d of Figure 4, a number of larger protrusions are visible in addition to the two species visible in parts a and b. These are closely spaced high molecular features and will be discussed in detail in a future publication.
(24) Hamers, R. J.; Demuth, J. E. *Phys. Rev. Lett.* **1988**, *60*, 2527.
(25) Frederick, B. G.; Leibsle, F. M.; Haq, S.; Richardson, N. V. *Surf. Rev. Lett.* **1996**, *3*, 1523.
(26) Lukas, S.; Witte, G.; Woll, Ch. *Phys. Rev. Lett*. **2002**, *88*, 028301.
(27) Kevan, S. *Phys. Rev. B* **1983**, *28*, 4822.
(28) Wu, D. Y.; Hayashi, M.; Chang, C. H.; Liang, K. K.; Lin, S. H. *J. Chem. Phys*. **2003**, *118*, 4073.
(29) Zhu, X.-Y. *Surf. Sci. Rep*. **2004**, *56*, 1.